Design and performance evaluation of a dispersion compensation unit using several chirping functions in a tanh apodized FBG and comparison with dispersion compensation fiber

Nazmi A. Mohammed,[1,3] Mohammad Solaiman,[1,*] and Moustafa H. Aly[2]

[1]Research Center, Smart Village, Arab Academy for Science, Technology, and Maritime Transport, Cairo, Egypt

[2]College of Engineering and Technology, Arab Academy for Science, Technology, and Maritime Transport, Alexandria, Egypt

[3]e-mail: naz_azz@aast.edu

*Corresponding author: msolaiman3100@gmail.com

Received 17 April 2014; revised 1 September 2014; accepted 2 September 2014;
posted 4 September 2014 (Doc. ID 210119); published 3 October 2014

In this work, various dispersion compensation methods are designed and evaluated to search for a cost-effective technique with remarkable dispersion compensation and a good pulse shape. The techniques consist of different chirp functions applied to a tanh fiber Bragg grating (FBG), a dispersion compensation fiber (DCF), and a DCF merged with an optimized linearly chirped tanh FBG (joint technique). The techniques are evaluated using a standard 10 Gb/s optical link over a 100 km long haul. The linear chirp function is the most appropriate choice of chirping function, with a pulse width reduction percentage (PWRP) of 75.15%, lower price, and poor pulse shape. The DCF yields an enhanced PWRP of 93.34% with a better pulse quality; however, it is the most costly of the evaluated techniques. Finally, the joint technique achieved the optimum PWRP (96.36%) among all the evaluated techniques and exhibited a remarkable pulse shape; it is less costly than the DCF, but more expensive than the chirped tanh FBG.

OCIS codes: (060.0060) Fiber optics and optical communications; (060.3735) Fiber Bragg gratings.
http://dx.doi.org/10.1364/AO.53.00H239

1. Introduction

Optical fibers have been used to meet the urgent demands for very high data transfer rates resulting from wide use of the Internet, electronic commerce, multimedia, PDAs, and telecommunications [1].

Three main obstacles restrict the rapid growth of system bandwidth: losses, nonlinear effects, and dispersion. Dispersion in particular is considered the major limiting factor for long-haul optical links. It severely degrades the performance of optical long-haul systems, decreases the cable length, limits the ability to achieve a remarkable bit rate, and also increases the bit error rate [1,2]. Several techniques have been proposed and evaluated to achieve effective dispersion compensation. The most important of these are the dispersion compensation fiber (DCF) [3–5], dispersion-compensating filter [6], high-order mode fibers [7], and fiber Bragg grating (FBG) [8].

Among these, the FBG has attracted huge interest for the design, testing, and evaluation of dispersion compensation units, as its effectiveness is due mainly to its complete passiveness, compactness, relatively low cost, low insertion loss, fiber compatibility, and lack of nonlinear effects [8]. Note that FBG is used in a huge range of optical telecommunication applications other than dispersion compensation, such as

1559-128X/14/29H239-09$15.00/0

fiber laser reflectors [9,10], wavelength division multiplexing (WDM) devices [11], optical pulse compression [12], tunable optical delay [13], optical filters [14,15], optical signal generation/shaping [16–18], and optical sensors [19,20].

As noted above, the DCF is an effective dispersion compensation technique. Previous studies have investigated the design and optimization of the DCF [21,22], the optimum DCF length choice for dispersion compensation [23,24], and the optimum operating conditions and application of the DCF as a dispersion compensation unit on several system structures/specifications [22,25] in detail.

Returning to the FBG as a dispersion compensator, a chirp modification should be introduced to obtain a chirped FBG (CFBG) [26]. Several related issues are addressed in the literature, such as designing the CFBG [27], optimizing the FBG parameters (i.e., grating length, refractive index modulation) [8], and applying the CFBG to single/WDM system structures [8].

Apodization functions can also add useful features to the CFBG, enhancing the dispersion compensation performance. They offer significantly improved sidelobe suppression, smooth the reflection spectrum, and provide a narrow bandwidth [26].

Linear chirping is the only chirp technique used in designing CFBGs as dispersion compensators in previous studies. While several apodization functions were introduced to improve the performance of CFBGs as a dispersion compensation unit [27,28], few studies indicated that tanh apodization should provide better dispersion compensation than other apodization profiles [28,29]. This technique is characterized by the sharpness of its grating edge and length, which results in a high linear time delay with minimum linear dispersion [28,29].

In this work, the application of well-known chirping techniques (square and cubic) to tanh apodization of the FBG is introduced, analyzed, and tested. A comparison with the standard linear CFBG is made.

Three dispersion compensation units are evaluated using a standard 10 Gb/s optical link with 100 km of SMF-28. Next, the performance of dispersion compensation units consisting of a DCF, or a DCF combined with the optimized chirped tanh FBG, is evaluated and compared. The comparison targets the PWRP, pulse quality, and cost.

This work is organized as follows. Section 2 presents the mathematical model, and Section 3 describes the system structure and specifications. The results and discussion are represented in Section 4, followed by the conclusion in Section 5.

2. Mathematical Model

A. Uniform FBG

The FBG has a refractive index that is spatially periodic along the light propagation (longitudinal) axis, as shown in Fig. 1. This profile can be created by exposing a photosensitive fiber to an ultraviolet light beam.

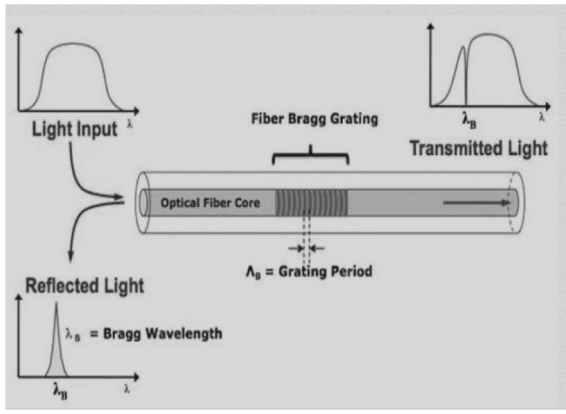

Fig. 1. Uniform FBG.

The FBG is well known for its use as a filter. Its application as a filter is usually described by [19]

$$\lambda_B = 2n_{\text{eff}}\Lambda_B, \tag{1}$$

where λ_B is the reflected wavelength (called the Bragg wavelength), n_{eff} is the effective refractive index of the fiber core at the free space center wavelength, and Λ_B is the grating period of the fiber.

B. Chirped FBG

For use in dispersion compensation, the FBG needs to be changed to a chirped structure. The CFBG is characterized by a nonuniform grating period, as shown in Fig. 2 [30]. The CFBG is a sequence of gratings with different periods that can reflect a range of wavelengths; this creates a distinct time delay for each wavelength [31]. The range of reflected wavelengths is provided by [13]

$$\Delta\lambda_{\text{chirp}} = 2n_{\text{eff}}(\Lambda_L - \Lambda_s) = 2n_{\text{eff}}\Delta\Lambda_{\text{chirp}}, \tag{2}$$

where λ_L is the longest wavelength, λ_S is the shortest wavelength, $\Delta\lambda_{\text{chirp}}$ is the difference between λ_L and λ_S, Λ_L is the longest grating period, and Λ_S is the shortest grating period.

A dispersion-broadened pulse is recompressed by letting the fast wavelengths of the pulse reflect from the shortest grating period in the chirp taking the longest time. In contrast, the slow wavelengths reflect from the longest one taking the shortest time, as shown in Fig. 2.

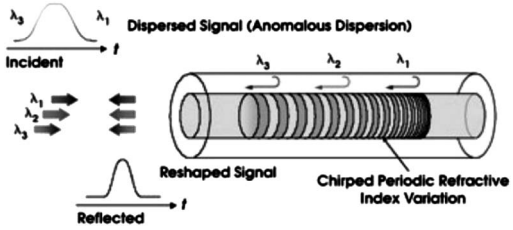

Fig. 2. CFBG.

According to an earlier concept, the CFBG compensates for greater dispersion as the number of gratings increases. Different wavelengths are reflected from different parts of the grating and are, accordingly, delayed by different amounts of time, as described by Eq. (3) for each wavelength. The reflection time delay of a CFBG is a function of the wavelength. The time delay, $\tau(\lambda)$, is given by [32],

$$\tau(\lambda) = \frac{(\lambda - \lambda_s)}{(\lambda_L - \lambda_s)} \frac{2n_{\text{eff}} L_g}{c} \qquad (\lambda_s \le \lambda \le \lambda_L), \tag{3}$$

where c is light speed in space and L_g is the grating length.

The anticipated result is a compression of the input pulse that can be modified to compensate for the dispersion accumulated down the link.

C. Chirp Profiles

Three specific chirping profiles have been extensively studied: the linear, square root, and cubic root profiles [33]. They are defined as follows:

Linear chirp,

$$\Lambda(z) = \Lambda_o - [(z - L_g/2)/L_g]\Delta. \tag{4}$$

Square root chirp,

$$\Lambda(z) = \Lambda_o - \left[\sqrt{z/L_g} - 1/\sqrt{2}\right]\Delta. \tag{5}$$

Cubic root chirp,

$$\Lambda(z) = \Lambda_o - \left[\sqrt[3]{z/L_g} - 1/\sqrt[3]{2}\right]\Delta. \tag{6}$$

Here, $\Lambda(z)$, Λ_o, and Δ represent the grating period at a distance, z, from the beginning of the grating, the grating period at the middle of the grating, and the total chirp, respectively.

D. Apodized CFBG

Applying certain functions, such as a Gaussian, sinc, and tanh, to create refractive index modulation $[\Delta n(z)]$ in the fiber core is known as apodization and is described by Eq. (7). A uniform FBG or CFBG with a rectangular refractive index modulation profile ($f_{\text{apodized}} = 1$, i.e., abrupt change) is not suitable for dispersion compensation. This is mainly because, in standard uniform Bragg gratings, the refractive index changes along the grating length are constant. Thus, they begin abruptly and end abruptly, yielding a sudden step change in the refractive index. The Fourier transform of this rectangular function is the well-known sinc function, with its associated sidelobe structure in the reflection spectrum. In a vast number of applications, such as WDM, it is very important to minimize and, if possible, to eliminate the reflectivity of these sidelobes [31].

The induced refractive index perturbation, Δn, is given by

$$\Delta n(z) = \Delta n f_{\text{apodized}}/n_{\text{eff}}, \tag{7}$$

where f_{apodized} is a function describing the refractive index modulation profile.

The term apodization refers to grading of the refractive index to approach the zero point at the end of the grating. The gradual increase in the refractive index modulation (introduced by apodization functions) from the tips toward the FBG center offers significantly improved sidelobe suppression, while it maintains the reflectivity and narrow bandwidth [26]. This makes apodization an essential design technique for making uniform FBG or CFBGs suitable for effective optical signal processing applications, including dispersion compensation [19].

The tanh profile used throughout this work is given by

$$T(z) = \tanh(\alpha \cdot z/L) \cdot \tanh[\alpha \cdot (1 - z/L)] + 1 - \tanh^2(\alpha/2), \tag{8}$$

where α is the tanh parameter.

To illustrate the discussion above, Figs. 3(a) and 3(b) clearly show that adding tanh apodization to the CFBG significantly improves the sidelobe suppression compared to that of the uniform CFBG while maintaining the reflectivity and narrow bandwidth.

E. DCF

When a DCF is used for dispersion compensation in a system built on single-mode fiber (SMF), the condition for perfect dispersion compensation is [34]

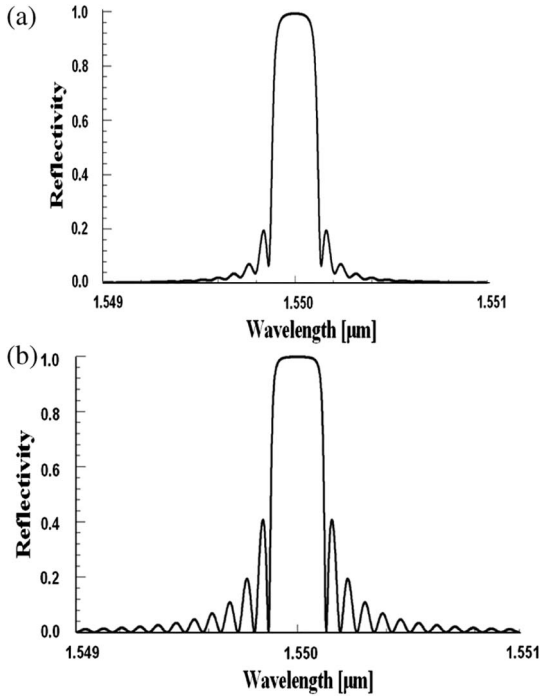

Fig. 3. (a) Normalized reflectivity spectrum of tanh CFBG and (b) normalized reflectivity spectrum of uniform CFBG.

$$L_1D_1 + L_2D_2 = 0, \quad (9)$$

where D_1 and D_2 are the fiber dispersions of the SMF and DCF, respectively, and L_1 and L_2 are the fiber lengths of the SMF and DCF, respectively.

3. System Structure and Specifications

A. Introduction

In this section, the optical system that will be used to test the performance of the ACFBG and DCF (separately and jointly) as a dispersion compensation unit is presented. The single-channel 10 Gb/s optical fiber system is shown in Fig. 4. The system consists of the optical transmitter, fiber cable, ACFBG and DCF acting as a dispersion compensation unit, optical amplifier [with an erbium-doped fiber amplifier (EDFA) as a preamplifier], and receiver.

The optimum parameters used to design tanh FBGs with different chirp functions (linear, square, or cubic) are numerically extracted from reflectivity studies using the mathematical model of Section 2. The parameters are then used to create a tanh FBG with these chirp functions as dispersion compensation units. Next, the system is established using a system simulator. Finally, the different chirp functions, as applied to a tanh FBG, DCF, and DCF merged with the optimized tanh CFBG, are tested and evaluated in the system as dispersion compensation units.

B. System Blocks

1. *Transmitter*

The transmitter (Tx) consists of a continuous wave (CW) laser source with a wavelength of 1553.9 nm (193.1 THz) and an output power of 1 mW [35]. It is externally modulated at 10 Gb/s with a non-return-to-zero (NRZ) [36] pseudorandom binary sequence in a Mach–Zehnder modulator with a 30 dB extinction ratio. The generated pulse has an initial width of 100 ps [37]. The transmitter block diagram is shown in Fig. 5.

2. *Optical Fiber*

An SMF (SMF-28) is used to test the performance of the dispersion compensation unit in the system shown in Fig. 4. The specifications of this fiber were

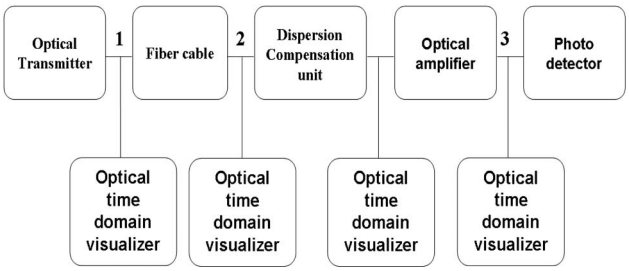

Fig. 4. Proposed system used to evaluate different dispersion compensation techniques.

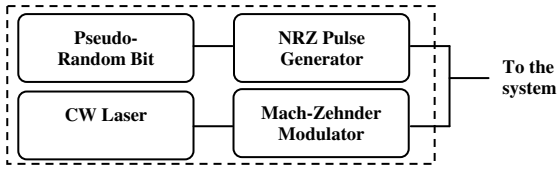

Fig. 5. Optical transmitter.

obtained from the vendors and are listed in Table 1 [36,38].

3. *Dispersion Compensation Unit*

a. *ACFBG*

The parameters used to design the ACFBG used as the first technique for dispersion compensation as described in Section 2 are tabulated in Table 2 [30,33,39]. The grating length is selected from the mentioned range to provide optimum dispersion compensation performance according to the technique used, as will be shown later.

b. *Dispersion Compensation Fiber*

The parameters of the DCF used as the second technique for dispersion compensation are tabulated in Table 3 [40].

4. *Optical Amplifier*

In this system, an EDFA with a 20 dB gain, which is independent of the wavelength, is used as a preamplifier [41].

5. *Photodetector*

The PIN specifications are tabulated in Table 4 [33,42].

Table 1. SMF Parameters

Dispersion (ps/km/nm) at 1550 nm	17
Dispersion slope (ps/nm^2/km) at 1550 nm	0.058
Length of fiber (km)	100
Attenuation index (dB/km)	0.20

Table 2. Designed ACFBG Parameters

Effective refractive index	1.45
Length of grating (mm)	70 mm (up to 100 mm)
Apodization function	Tanh
Tanh parameter	1–4
Chirp parameter	0.0007

Table 3. DCF Parameters

Dispersion (ps/km/nm) at 1550 nm	−80
Dispersion slope (ps/nm^2/km) at 1550 nm	−0.3
Attenuation index (dB/km)	0.5

Table 4. PIN Specifications

Dark current (nA)	10
Thermal noise coefficient (W/Hz)	2.048e – 23
Responsivity (A/W)	1

4. Results and Discussion

A. Introduction

In this section, the system proposed in Section 3.A will be used to test and evaluate three different dispersion compensation techniques: the designed ACFBG only, the DCF only, and both of these techniques together, as described in Sections 4.B, 4.C, and 4.D, respectively. In Section 4.E, a detailed comparison will be carried out to determine the optimum technique(s) that would be most suitable for dispersion compensation. Furthermore, the cost effectiveness will be considered.

Before the results are introduced, it should be noted that the major concern of this work is to identify the level of dispersion compensation achieved by each technique. An effective way to do this is by defining what is called the pulse width reduction percentage (PWRP).

The PWRP is described as follows. Assuming that the pulse is sent with a pulse width of z from the transmitter and undergoes dispersion as it travels through the fiber link, resulting in a broadened pulse with a width of y, and that the pulse width of the signal after the dispersion compensation unit is x, then the PWRP can be calculated as $[(y-x)/(y-z)]$.

Other, less important, evaluation parameters, such as the signal amplitude after the optical amplifier and the pulse after traveling through the fiber (with width y), can be extracted directly from the figures in the following subsections.

B. Dispersion Compensation Using ACFBG

1. *Introduction*

In this section, the system introduced in Section 3.A will be used to evaluate the designed ACFBG as a dispersion compensation unit. A trace for the labeled points (1, 2, and 3) in Fig. 4 of Section 3.A will be presented and analyzed.

The chirping functions in the AFBG (Table 2) will be evaluated by investigating their effects on the dispersion compensation levels.

2. *System Trace and Results*

The input signal at point 1 (according to the specifications in Section 3.B.1) is shown in Fig. 6. In Fig. 7, the output at point 2 is depicted, showing the effect of fiber dispersion on the signal; the signal is broadened from 100 to 265 ps with perturbations in the spectrum, and the power level is attenuated to 10 μW.

Figure 8 shows the signal at point 3 in Fig. 4. It compares the dispersion compensation performance of the AFBG with linear, square, and cubic chirp functions. The results were obtained using the predetermined specifications in Section 3.B.3. By numerical trials and using this technique only as a dispersion compensation unit, acceptable dispersion compensation performance is achieved by setting $L_g = 50$ mm and the chirp parameter to 0.0003 in all the chirping functions. In addition, using this value makes it possible to compare the performance of different types of chirp function.

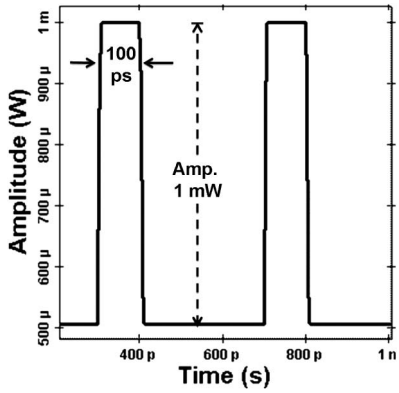

Fig. 6. Input pulse (point 1, Fig. 4).

When a linear chirp function is applied to the AFBG, a 75.15% PWRP is achieved, yielding a 141 ps signal with an amplitude of 944 μW, as shown in Fig. 8(a). For the square root chirp function, the AFBG exhibits a fair PWRP of 72.72%, yielding a 145 ps signal with an amplitude of 985 μW, as shown in Fig. 8(b). Finally, using the cubic root ACFBG yields the worst PWRP. In Fig. 8(c), a PWRP of only 43.63% was observed, for a broadened signal of 193 ps. The maximum measured signal amplitude is 996 μW. Note that the cubic chirp is the optimum choice in terms of the signal amplitude after the optical amplifier. Small gain amplitudes of 11 and 52 μW for the square root and linear chirp, respectively, are observed.

The obtained results can be understood using Eqs. (4)–(6), assuming that z reaches its maximum allowable value, L_g. One can detect that Λ (L_g) becomes greater when the chirp function changes from linear to cubic. This leads to the creation of small periods with linear chirping and then to larger periods for square and cubic chirping. Therefore,

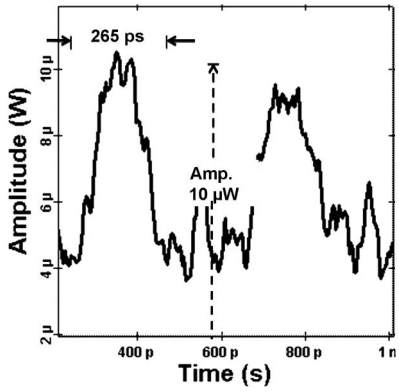

Fig. 7. Signal after 100 km of SMF (point 2, Fig. 4).

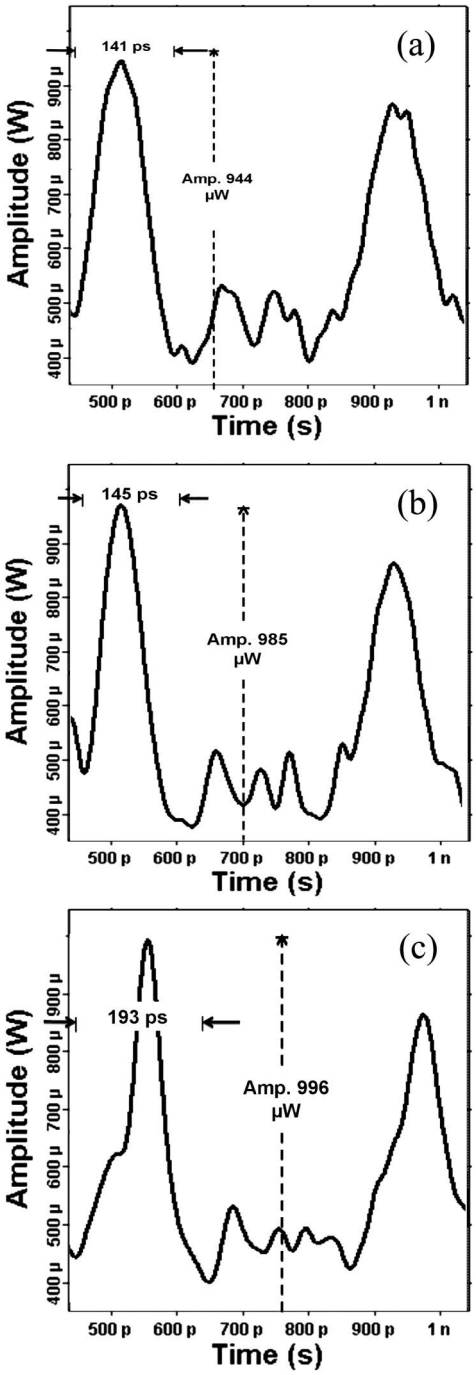

Fig. 8. Performance of (a) linearly chirped AFBG, (b) square-chirped AFBG, and (c) cubic-chirped AFBG as a dispersion compensation unit (point 3, Fig. 4, after optical amplifier).

the linear chirp function reflects more wavelengths than the square and cubic roots, resulting in the best dispersion compensation performance. This concept agrees fairly well with the theoretical investigation in Section 2.B.

C. Dispersion Compensation Using DCF

1. *Introduction*

In this section, the common, well-known technique for dispersion compensation (the DCF) will be used as a dispersion compensation unit in the system presented in Fig. 4. The system specification used to test the designed tanh CFBG in Section 4.B will be applied here. The dispersion compensation performance will be evaluated.

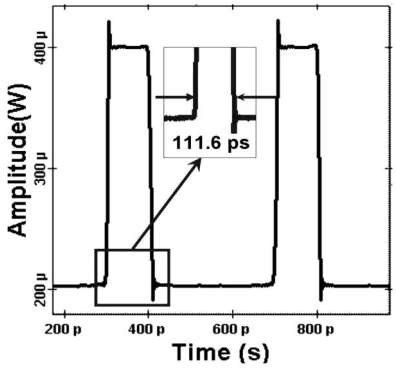

Fig. 9. Signal after DCF (point 3, Fig. 4, after optical amplifier).

2. *Results*

Again, the input signal (at point 1 in Fig. 4) and the signal after 100 km of transmission (at point 2 in Fig. 4) appear in Figs. 6 and 7, respectively. The parameters of the DCF in Table 3 are applied. Using the mathematical model (Section 2.E) and the specifications of the proposed system, one can predict that the DCF will yield the optimum dispersion compensation performance with a length of 21.25 km.

The results agree fairly well with the mathematical model. Figure 9 shows that excellent dispersion compensation performance was observed after 20.93 km of DCF (point 3, Fig. 4). A PWRP of 93.34% on the dispersed signal (shown in Fig. 7) is observed, and the signal width reaches 111.6 ps, as shown in Fig. 9. Another observation is that the shape of the signal after dispersion compensation using the optimum length of the DCF is better than that observed by the designed tanh CFBG. Fig. 10 shows the PWRP for DCF lengths other than the optimal value; this information will be discussed in terms of the cost of using this technique in Section 4.E.

D. Dispersion Compensation Using DCF + ACFBG

1. *Introduction*

In this section, the DCF and the optimized tanh CFBG (linearly chirped according to Section 4.B) will

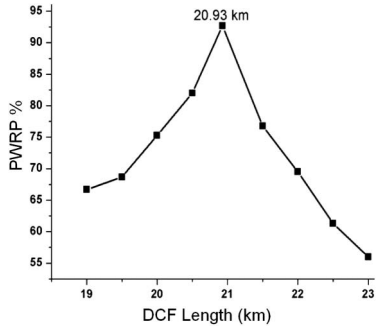

Fig. 10. PWRP achieved by DCF.

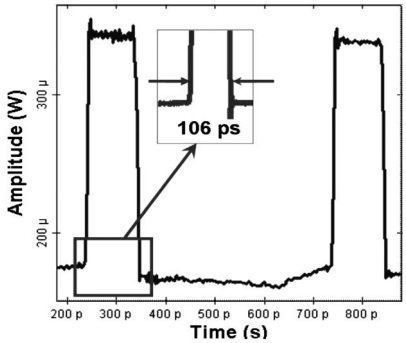

Fig. 11. Signal after amplifier and optimum DCF length merged with linearly chirped tanh FBG for dispersion compensation (point 3, Fig. 4, after optical amplifier).

be used together as a dispersion compensation unit in the system shown in Fig. 4. All the specifications of the DCF and the linearly chirped tanh FBG are the same as in Section 3.B.3. The system specifications used to test the DCF and the designed linearly chirped tanh FBG individually in the previous two sections will be applied here.

2. *Results*

After numerical trials using the provided mathematical model to obtain the maximum dispersion compensation performance using this joint technique, the grating length of the designed linearly chirped tanh FBG was set to 70 mm. The results reveal that merging the DCF and the linearly chirped tanh FBG will provide the optimum dispersion compensation performance among the three techniques. A remarkable PWRP of 96.36% on the dispersed signal shown in Fig. 7 is observed, for a signal width of 106 ps, as shown in Fig. 11. This is associated with a reduction of the required DCF length by 4.18 km (to 16.75 km) compared to the value in Section 4.C. This joint technique retains a good pulse shape compared to that observed for the DCF technique alone. Fig. 12 shows the PWRP for various DCF lengths using the joint technique.

E. Comparison of Techniques and Cost-Related Issues

In this section, the optimized linearly chirped tanh FBG, the DCF, and the DCF with the linearly chirped tanh FBG are compared. The comparison is based on the PWRP achieved with each technique, the length of the DCF required to achieve the maximum obtained PWRP for the proposed system, the optimum grating length, and the pulse quality. Table 5 summarizes these points for the tested techniques, with an emphasis on the cost-related issues.

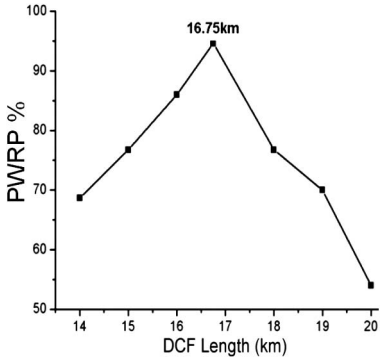

Fig. 12. PWRP as a function of DCF length for a combination of DCF with linearly chirped AFBG.

Table 5. Comparison of Discussed Techniques

Technique	ACFBG	DCF	DCF with ACFBG
PWRP	75.15%	93.34%	96.36%
Shape of pulse after compensation. (pulse quality)	Poor	Good	Fair
Grating length	50 mm	—	70 mm
DCF length	—	20.93 km	16.75 km
Cost	Lowest	High	Lower than that of DCF only

Regarding the performance of the dispersion compensation unit, the DCF together with the linearly chirped tanh FBG achieves the maximum PWRP with an acceptable pulse quality (after dispersion compensation and amplification). The FBG technique has the lowest cost among all the techniques discussed here. However, this work generally indicates that this low cost is associated with the low dispersion compensation performance (PWRP and pulse quality).

This performance may be acceptable when linear chirping is used, but the problem of poor pulse shaping (quality) should be addressed.

This work also indicates that the DCF acts as an excellent dispersion compensation unit, yielding a PWRP of 93.34% and a remarkable pulse shape (quality) after dispersion compensation and amplification. However, this performance is associated with the high cost required to achieve that PWRP ($3 per meter of DCF for −38 ps/nm · km) [43]. Note that the DCF used in this work has −80 ps/nm · km and will cost more per meter.

Finally, the DCF combined with the optimized linearly chirped tanh FBG achieves the best PWRP among all the techniques. A very good pulse shape (quality) is observed after compensation and amplification. This combined technique is expected to cost less than the DCF technique because adding the linearly chirped tanh FBG saves 4.18 km of DCF length.

A survey of vendors revealed that using only the DCF as a dispersion compensation technique is the most expensive among all the investigated techniques. Using only the CFBG as a dispersion compensation technique can reduce the dispersion compensation unit cost by about 98% compared to the DCF cost, considering the previously mentioned drawbacks (i.e., the low PWRP and pulse quality). In summary, the proposed combined dispersion compensation technique is expected to yield a saving of about 15% of the dispersion compensation unit cost compared to the DCF cost but with a huge enhancement in the dispersion compensation performance:

the optimum PWRP among the techniques investigated here and a reasonable pulse shape (quality).

5. Conclusion

This work experimentally and numerically tested a single-channel system using standard values and equipment to evaluate the dispersion compensation performance of several dispersion compensation techniques. The results show that linear chirping is preferable among all the chirping functions for dispersion compensation purposes. The study indicates that the grating length should be optimized to guarantee acceptable dispersion compensation behavior. The DCF technique yields a good dispersion compensation unit, but it is costly for the standard link in the system under examination. The DCF, together with the optimized linearly chirped tanh FBG, achieves remarkable dispersion compensation performance that is associated with an acceptable pulse shape, and its price is moderate.

The authors are grateful to Bob Chomycz of Telecom Engineering, Inc., for supplying useful information regarding the FBG specs, Eng. Taha A. Ali for his kind help and information, Eng. Tamer F. Ismail for providing language help, and Dr. Yosra M. Akl for her advice and proofreading assistance.

References

1. J. M. Senior and M. Y. Jamro, *Optical Fiber Communications: Principles and Practice* (Pearson Education, 2009).
2. C. P. Yu, J. H. Liou, S. S. Huang, and H. C. Chang, "Tunable dual-core liquid-filled photonic crystal fibers for dispersion compensation," Opt. Express **16**, 4443–4451 (2008).
3. J. L. Auguste, R. Jindal, J. M. Blondy, M. Clapeau, J. Marcou, B. Dussardier, G. Monnom, D. B. Ostrowsky, B. P. Pal, and K. Thyagarajan, "–1800 ps/(nm·km) chromatic dispersion at 1.55 μm in dual concentric core fibre," Electron. Lett. **36**, 1689–1691 (2000).
4. L. G. Nielsen, S. N. Knudsen, B. Edvold, T. Veng, D. Magnussen, C. C. Larsen, and H. Damsgaard, "Dispersion compensating fibers," Opt. Fiber Technol. **6**, 164–180 (2000).
5. K. Pande and B. P. Pal, "Design optimization of a dual-core dispersion-compensating fiber with a high figure of merit and a large effective area for dense wavelength-division multiplexed transmission through standard G.655 fibers," Appl. Opt. **42**, 3785–3791 (2003).
6. K. Takiguchi, K. Okamato, and K. Moriwaki, "Planar lightwave circuit dispersion equalizer," IEEE Photon. Technol. Lett. **6**, 86–88 (1994).
7. A. H. Gnauck, L. D. Garrett, Y. Danziger, U. Levy, and M. Tur, "Dispersion and dispersion-slope compensation of NZDSF over the entire C band using higher-order-mode fibre," Electron. Lett. **36**, 1946–1947 (2000).
8. M. Sumetsky and B. J. Eggleton, "Fiber Bragg gratings for dispersion compensation in optical communication systems," in *Journal of Optical and Fiber Communication Reports 2* (Springer-Verlag, 2005) pp. 256–278.
9. X. Cheng, C. H. Tse, P. Shum, R. F. Wu, M. Tang, W. C. Tan, and J. Zhang, "All-fiber Q-switched erbium-doped fiber ring laser using phase-shifted fiber Bragg grating," J. Lightwave Technol. **26**, 945–951 (2008).
10. K. Sakai, S. Itakura, N. Shimada, K. Shibata, Y. Hanamaki, T. Yagi, and Y. Hirano, "High-power tapered unstable-resonator laser diode with a fiber-Bragg-grating reflector," IEEE Photon. Technol. Lett. **21**, 1103–1105 (2009).
11. Q. Wu, P. Chu, and H. Chan, "General design approach to multichannel fiber Bragg grating," J. Lightwave Technol. **24**, 4433–4454 (2006).
12. Q. Li, P. Wai, K. Senthilnathan, and K. Nakkeeran, "Modeling self-similar optical pulse compression in nonlinear fiber Bragg grating using coupled-mode equations," J. Lightwave Technol. **29**, 1293–1305 (2011).
13. H. Shahoei, M. Li, and J. Yao, "Continuously tunable time delay using an optically pumped linear chirped fiber Bragg grating," J. Lightwave Technol. **29**, 1465–1472 (2011).
14. Y. Gong, X. Liu, L. Wang, X. Hu, A. Lin, and W. Zhao, "Optimal design of multichannel fiber Bragg grating filters with small dispersion and low index modulation," J. Lightwave Technol. **27**, 3235–3240 (2009).
15. Z. Li, V. Hsiao, Z. Chen, J. Tang, F. Zhao, and H. Wang, "Optically tunable fiber Bragg grating," IEEE Photon. Technol. Lett. **22**, 1123–1125 (2010).
16. C. Wang and J. Yao, "Fourier transform ultrashort optical pulse shaping using a single chirped fiber Bragg grating," IEEE Photon. Technol. Lett. **21**, 1375–1377 (2009).
17. Y. Dai and J. Yao, "Optical generation of binary phase-coded direct-sequence UWB signals using a multichannel chirped fiber Bragg grating," J. Lightwave Technol. **26**, 2513–2520 (2008).
18. C. Wang and J. Yao, "Photonic generation of chirped millimeter-ave pulses cased on nonlinear frequency-to-time mapping in a nonlinearly chirped fiber Bragg grating," IEEE Trans. Microw. Theory Techn. **56**, 542–553 (2008).
19. N. A. Mohammed, T. A. Ali, and M. H. Aly, "Evaluation and performance enhancement for accurate FBG temperature sensor measurement with different apodization profiles in single and quasi-distributed DWDM systems," Opt. Lasers Eng. **55**, 22–34 (2014).
20. N. A. Mohammed, T. A. Ali, and M. H. Aly, "Performance optimization of apodized FBG-based temperature sensors in ingle and quasi-distributed DWDM systems with new and different apodization profiles," AIP Adv. **3**(12), 1–21 (2013).
21. T. Tsuritani, N. Takeda, K. Imai, K. Tanaka, A. Agata, I. Morita, H. Yamauchi, N. Edagawa, and M. Suzuki, "1 Tbit/s (10 × 10.7 Gbit/s) transoceanic transmission using 30 nm wide broadband optical repeaters with Aeff-enlarged positive dispersion fibre and slope-compensating DCF," Electron. Lett. **35**, 2126–2128 (1999).
22. L. Grüner-Nielsen, "Dispersion-compensating fibers," J. Lightwave Technol. **23**, 3566–3579 (2005).
23. R. Nuyts, Y. Park, and P. Gallion, "Dispersion equalization of a 10 Gb/s repeatered transmission system using dispersion compensating fibers," J. Lightwave Technol. **15**, 31–42 (1997).
24. O. Arora and A. K. Garg, "Dispersion compensation for high speed optical networks," MIT Int. J. Electron. Commun. Eng. **2**, 1–4 (2012).
25. C. C. Chang and A. M. Weiner, "Fiber transmission for sub-500-fs pulses using a dispersion-compensating fiber," IEEE J. Quantum Electron. **33**, 1455–1464 (1997).
26. R. Romero, O. Frazão, F. Floreani, L. Zhang, P. V. S. Marques, and H. M. Salgado, "Chirped fibre Bragg grating based multiplexer and demultiplexer for DWDM applications," Opt. Lasers Eng. **43**, 987–994 (2005).
27. S. Wakabayashi, A. Baba, A. Itou, and J. Adachi, "Design and fabrication of an apodization profile in linearly chirped fiber Bragg gratings for wideband >35 nm and compact tunable dispersion compensator," J. Opt. Soc. Am. B **25**, 210–217 (2008).
28. E. J. Gualda, L. C. Gomez-Pavon, and J. P. Torres, "Compensation of third-order dispersion in a 100 Gb/s single channel system with in-line fibre Bragg gratings," J. Mod. Opt. **52**, 1197–1206 (2005).
29. S. Agarwal and V. Mishra, "Effect of grating length on chromatic dispersion in polymer coated apodization grating," IJRTE **2**(5), 36–39 (2013).
30. R. Kashyap, *Fiber Bragg Gratings* (Academic, 2010).
31. F. Karim and O. Seddiki, "Numerical analysis of raised cosine sampled chirped Bragg grating for dispersion compensation in dense wavelength division multiplexing systems," Int. J. Commun. **3**, 9–16 (2009).
32. Z. Zhang, "Passive and active Bragg gratings for optical networks," Ph.D. dissertation (University of Southampton, 2007).
33. M. R. Salehi, E. Abiri, M. Dezfouli, and K. Kazemi, "Mitigating the impact of group velocity dispersion in a time-spreading

optical CDMA system," in *Proceedings of the 5th International Symposium on Telecommunication* (2010), pp. 147–150.
34. H.-H. Lu, "Performance comparison between DCF and RDF dispersion compensation in fiber optical CATV systems," IEEE Trans. Broadcast. **48**, 370–373 (2002).
35. Y. Huang, J. P. Heritage, and B. Mukherjee, "Connection provisioning with transmission impairment consideration in optical WDM networks with high-speed channels," J. Lightwave Technol. **23**, 982–993 (2005).
36. S. K. Liaw, L. Dou, and A. Xu, "Fiber-Bragg-grating-based dispersion-compensated and gain-flattened Raman fiber amplifier," Opt. Express **15**, 12356–12361 (2007).
37. L. Banchi, M. Presi, A. D'Errico, G. Contestabile, and E. Ciaramella, "All-optical 10 and 40 gbit/s RZ-to-NRZ format and wavelength conversion using semiconductor optical amplifiers," J. Lightwave Technol. **28**, 32–38 (2010).
38. Z. Tan, Y. Wang, W. Ren, Y. Liu, B. Li, T. Ning, and S. Jian, "Transmission system over 3000 km with dispersion compensated by chirped fiber Bragg gratings," Optik **120**, 9–13 (2009).
39. K. Hsu, L. Sheu, K. Chuang, S. Chang, and Y. Lai, "Fiber Bragg grating sequential UV-writing method with real-time interferometric side-diffraction position monitoring," Opt. Express **13**, 3795–3801 (2005).
40. M. I. Hayee and A. E. Willner, "NRZ versus RZ in 10–40-Gb/s dispersion-managed WDM transmission systems," IEEE Photon. Technol. Lett. **11**, 991–993 (1999).
41. S. Pachnicke, M. Obholz, E. Voges, P. M. Krummrich, and E. Gottwald, "Electronic EDFA gain control for the suppression of transient gain dynamics in long-haul transmission systems," in *Optical Fiber Communication Conference* (Optical Society of America, 2007).
42. K. Preston, Y. Lee, M. Zhang, and M. Lipson, "Waveguide-integrated telecom-wavelengthphotodiode in deposited silicon," Opt. Lett. **36**, 52–54 (2011).
43. Thorlabs, Inc., http://www.thorlabs.de [accessed July 11, 2014].